The automatic classification of urban open space by a pattern-matching method of the viewshed at intersections

Thomas Leduc, Kevin Hartwell

The Automatic Classification of Urban Open Space by a Pattern-matching Method of the Viewshed at Intersections

Thomas LEDUC

AAU-CRENAU, UMR CNRS 1563, National School of Architecture of Nantes, France

Kevin HARTWELL

AAU-CRENAU, UMR CNRS 1563, National School of Architecture of Nantes, France

Abstract

This research focuses on the automatic classification of small urban fragments through a morphological analysis of cognitivist inspiration. The recognition algorithm is performed on observer-centric forms, constructed through the use of visibility assessment techniques over a series of individual points of view. These tools are 1) the isovist for its capacity to delineate and synthesize the visual properties of the immediate viewshed from a point, and 2) the automatic construction of a typology of intersection patterns. The aim is to assimilate the forms of the theoretical intersection patterns to those extracted from the isovist field generated by a group of strategically placed points. Three different matching methods are proposed, and the significance of the parameters needed for optimal calibration are discussed.

Key-words

Shape recognition, isovist field, pattern matching, Fourier transform, intersection

Introduction

Non-uniform representations of urban junctions

A comparison of the linear road data from Web Map service providers reveals that the treatment of intersections (nodes in the urban graph) is not a uniform procedure, thus

resulting in multiple interpretations. As an introductory illustration, the intersection of the Lecesne, Eyries, du Bastion and Delavigne Streets in Le Havre, France (49°29'36.4589", 0°7'0.0235") is one of many such crossroads (figure 1).

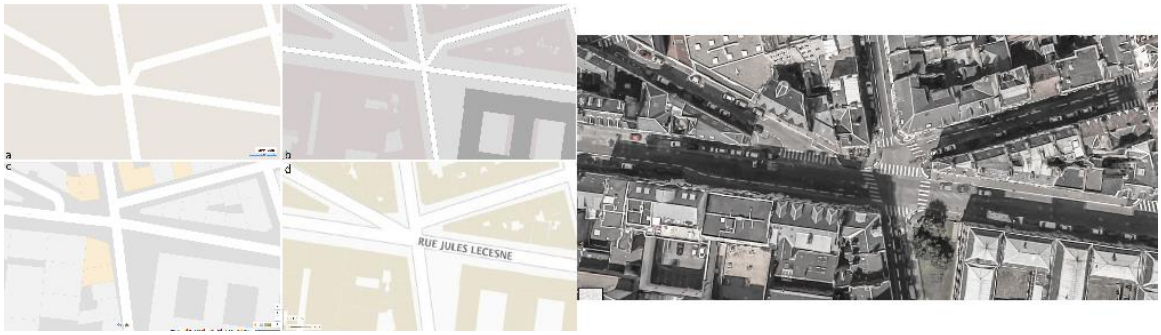

Figure 1: The Lecesne intersection as seen by: a) Bing; b) OpenStreetMap; c) Google Maps; d) Géoportail; e) Aerial View.

As can be seen, this zone is interpreted either as consisting of an eastern three-branch intersection and a western five-branch intersection (Bing Maps, figure 1a), a unique point with six branches (OpenStreetMap, Mappy, figure 1b), three distinct points (Google Maps, figure 1c), or two intersections with five branches for the southern point and three branches for the northern point (Géoportail, figure 1d).

A satellite view of the zone (figure 1e) reinforces the perceived complexity: a great number of concurring roads, a juxtaposition of acute and obtuse angles, atypical corner buildings creating mask effects, unconventional crosswalk positions, etc. The “ground truth” itself defies simple determination and consistent interpretation.

This divergence in representation exhibits the lack of consensus concerning the interpretation of this complex urban object. Although some dissimilarities may stem from differing linear road extraction methods, much of the issue concerning intersection point placement and characterization also lacks proper formalization. This variation has repercussions on cartographic representation, urban graph analysis, accurate positioning and wayfinding processing.

As the difference between “correct” and “incorrect” representations of a given intersection are difficult to distinguish, we may rather ponder how to consistently read and represent complex urban junctions.

Embracing the subjective quality of this urban object, our objective is to classify intersections according to their impact on their *in situ* cognitive repercussions.

From street patterns and building patterns to open space patterns

Within the framework of map generalization, whose objective is to group and simplify more or less complex geographical forms and phenomena, various studies exist that aim to automate the detection and simplification of junctions in road networks. The existing processes are based on a thinning of the road network, coupled with edge deletion and contraction mechanisms to reduce the complexity within the junction (Mackaness and Mackechnie, 1999). Their objective is clearly to produce schematic and meaningful visualizations in cartography.

In the same vein, we can mention the attempts of (Zhou and Li, 2012), who produced a “comparative study of various strategies to concatenate road segments into strokes for map generalization”. This abstraction level is sometimes useful for better understanding the structure of a road network.

Aforementioned studies should be distinguished from that on the accurate road centerline detection from satellite imagery in digital photogrammetry (Cao and Sun, 2014). As (Wang et al., 2016) points out, the most recent approaches incorporate knowledge-based methods that complement the extractions that were previously based on spectral and shape features without texture information. Some authors propose to couple the use of vector road data to remote sensing technology in satellite image detection to connect broken road segments. In most of these analyses, the levels of detail used are coarse and the objective aims to reconstruct and guarantee the topology of the street network.

This centerline-based approach does not handle large open spaces, as for instance squares. Thus, as can be seen from figure 2, the skeleton of a T-junction (figure 2a) is almost identical to the skeleton of an intersection leading to a square (figure 2b). It is de facto sometimes inadequate to reflect the complexity of some urban places.

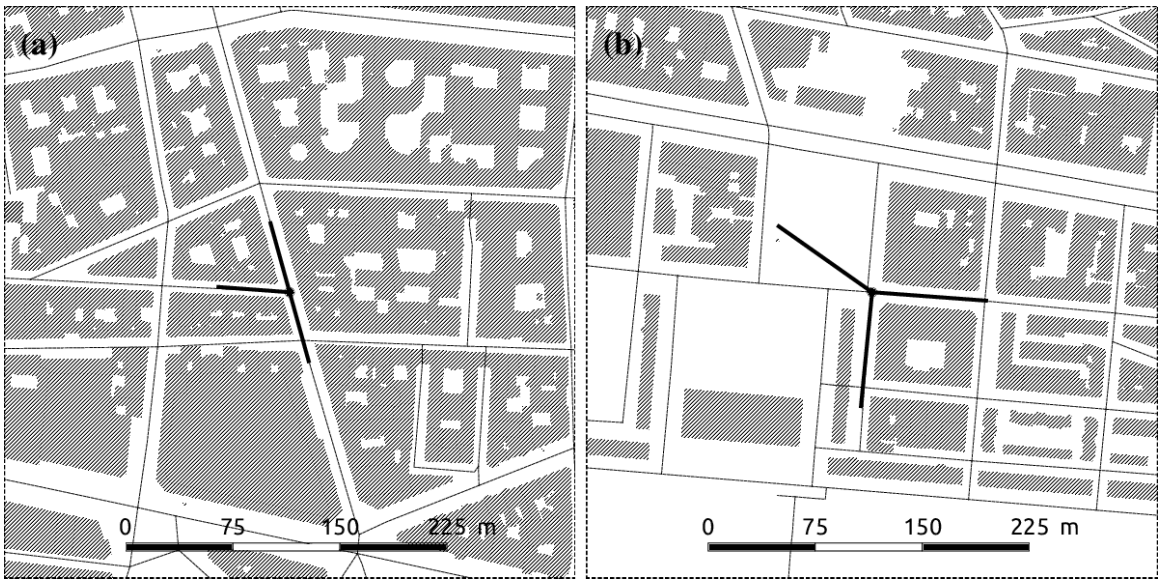

Figure 2: The detection of road intersections by the skeleton method does not take into account large open spaces, as for instance squares.

A number of these studies employ or mention the notion of "pattern" which corresponds to a repeating structural, spatial or temporal feature referring to a composition, configuration or constitution (Marshall, 2005). For example, (Zhang et al., 2011, 2017) have worked on "building pattern recognition" from topographic data by combining the results of multiple pattern-recognition algorithms.

In our present study, we question the representation of streetspace, the 2D open space that fits between buildings and forms the essential connective tissue of the city. As (Marshall, 2005) points out, "streetspace forms the basic core of all urban public space – and by extension, all public space – forming a contiguous network or continuum by which everything is linked to everything else".

This particular contiguity, the "plenum of the urban space" (Couclelis, 1992), renders the delineation and identification of localized objects such as intersections difficult. In contrast, (Teller, 2003) considers that atomist space conceives of the urban space as a reference system, where objects are identified and defined by their clear and

stable limits. These clearly definable objects may be transformed (through rotation, symmetry, translation, etc.) whilst retaining their identity.

The isovist as a solution to delineate the void between buildings

We have chosen the isovist field (Benedikt, 1979) which consists in immersing a theoretical panoptic view at a point into the urban numerical space. This point and its associated view constitute a translation of the perception of the microscale streetscape features that affect the *in situ* experience of the open space (Fisher-Gewirtzman, 2018). Essentially, isovists describe local geometrical properties of spaces with respect to individual observation points with an equal discretion for all possible view directions by forming a 2D horizontal slice of a pedestrian's viewshed of the surrounding space.

In the absence of any opaque surfaces, the limit of the isovist is an arbitrary artificial horizon. By giving form to an area around a point in the continuous field strictly defined by the radius of the isovist and the neighboring building footprints, the isovist may constitute an atomist reduction of the urban plenum.

This appealing concept offers an intuitively attractive analytical framework of a spatial environment, as it provides a description of the space from the point of view of individuals as they perceive, interact and move through it (Turner et al., 2001).

Positioning viewpoints

Intuitively but also for reasons of convenience and availability of dataset, we chose to analyze the road network and locate these viewpoints - the viewsheds generating points - at the road junctions. Nevertheless, as we will discuss later in this document, one must recognize that with such a solution, point placement is sometimes not optimal and that there is often a surplus of points for a single intersection area. Alternative solutions exist, such as skeletonization (Sarradin et al., 2007), which make it possible to minimize this number of points.

Visual patterns and geospatial patterns

(Steiniger, 2007) describes a "visual pattern" as a subjective, immersed recognizable form, and a "geo-spatial pattern" as an objective form constructed with full knowledge of

the terrain. (Ai et al., 2013) noticed that traditional spatial analysis concentrates on geo-spatial patterns, for example geometric, topologic or semantic information, but rarely relies upon cognition-related information, which would be here represented by visual patterns.

The isovist form, its central point of view (figure 3a, junction in road network) and resulting viewshed (figure 3b), hold the same characteristics as a "visual pattern" as defined by Steiniger. To classify these visual patterns, we posit that information extracted from the isovist mimics a synthetic, exterior view of the studied terrain.

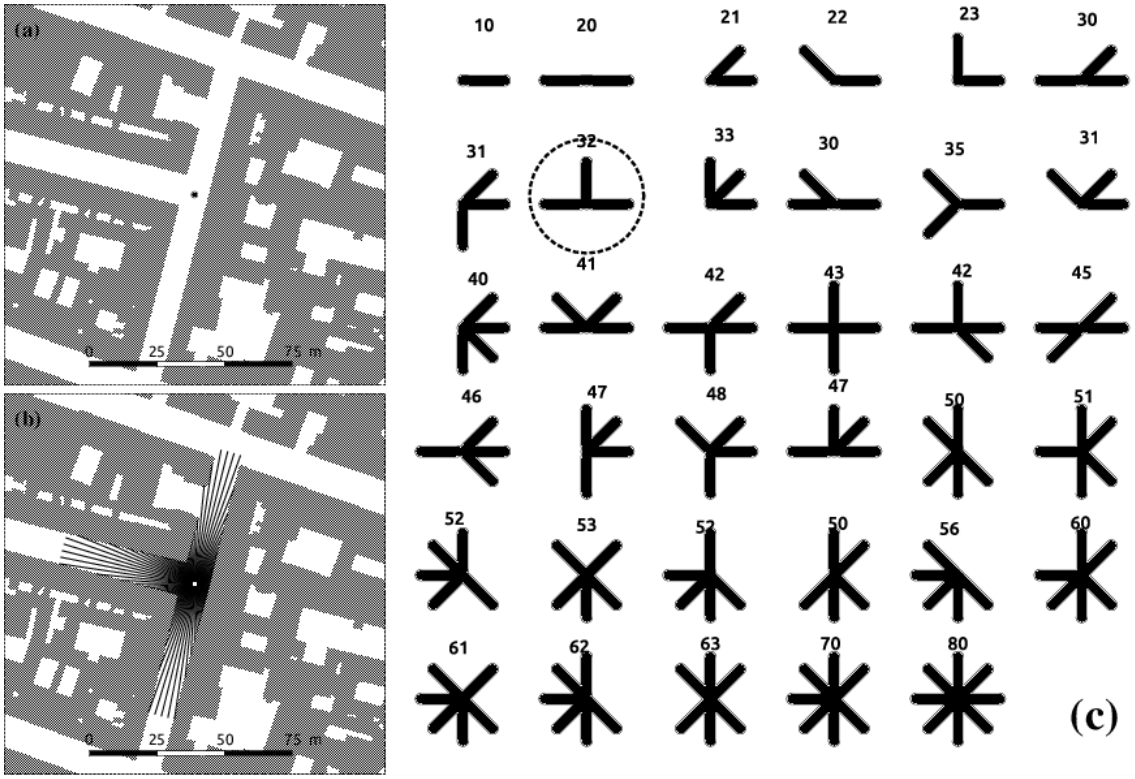

Figure 3: The isovist (b) created from a point of view (a) is similar to a purely geometric form (c).

Such similarities allow us to compare them to a series of objective intersection patterns (figure 3c). Such objective patterns can be associated with "geo-spatial pattern",

as they are created with specific domain knowledge, independent of any specific point of view. In other words, we may assimilate visual patterns to geo-spatial patterns by understanding the *in situ* visual repercussions of spatial configurations. Our objective is therefore to match the cognition-related information (visual patterns captured *in situ*) with geospatial patterns that have been arbitrarily predefined.

After presenting the isovist as a solution for the atomization of plenum space, the decomposition of its resulting form into a function of radial distances is explained, followed by the methodology for the automatic construction of reference patterns. After the description of the three pattern recognition methods, three case studies are then presented illustrating the impact of the urban morphologies on the results obtained. Case study results allow us to draw conclusions regarding the parameters affecting the quality of the process.

Methods

Isovist form as a function of radial distances

The isovist is a visibility polygon, meaning all segments from the generation or view point to all other points within the shape lie entirely within the polygon. Taking advantage of this star-shaped property, we can derive a shape signature based on the generation point and its correspondent boundary. This dimensionality reduction solution limits the study of the form to that of its contour which is sampled at their intersection with a series of equally-angled segments (rays) originating from the center point.

This angular abscissa sampling solution allows us to transform the 2D-polygonal surface into a simple 1D-function of a real variable that, at a given azimuth (θ_k), returns the associated ray length (r_k). Let n be the number of rays, using complex number formalism and Euler's number (e), the k-ray can be represented as:

$$r_k e^{i\theta_k} = r_k e^{i\frac{2\pi k}{n}}$$

Since this shape signature is only dependent on the location of the viewpoint and the points on the boundary, it sits in a local coordinate system and is thus invariant to translation in space. The matchmaking between the isovist form and a reference pattern is therefore independent from the viewpoint's localization on the map.

The radial “sweep” is systematically operated from 0° to 360° starting full East, in the counterclockwise direction. This means the function of radial distances is dependent on the local orientation of the intersection.

Pattern generation

The form-generating model that we have developed for the construction of our reference (or geo-spatial) patterns is entirely automatic, based on the principles of permutation of a “word”, that “word” being the mechanism that allows us to encode the intersection.

Based on this formal definition of words, we may generate the figure 3c, representing all possible intersection forms having at most 8 branches separated by steps of 360/8=45°. Patterns equivalent with regards to the mirror effect share the same IDs.

A limit of eight branches was selected, as multiples of four include the most frequent angularity (90°) which a multiple of 5 for example would not. The number of possible branches exponentially increases the number of patterns, which reduces the distinguishability (i.e., distance) between patterns with relatively superfluous differences, greatly complicating the manual assessment. As complementary information, one can notice that with a maximum of 4 branches (resp. 8, 12, and 16), one may generate 13 different patterns (resp. 35, 351, and 4115).

Patterns were created by casting the rays corresponding to their encoding, then buffering the resulting multilinear geometry. The *width* parameter describes the buffer breadth used during the pattern construction. This has ulterior consequences on pattern matching for methods using the Fourier Transform, as it dictates the quantity of uninterrupted open space considered for a single branch. If a branch is much larger than the arbitrary width, Method 2 identifies it as two branches. Inversely, if the chosen width is significantly larger than the real-world branch, it might be overlooked. Optimal widths for our chosen case studies are 14m (New York) and 10m (Paris, Le Havre).

Pattern matching process: methodology overview

The strategies set in place to judge of the similarity are based on different mathematical principles. The first method uses the turning angle function’s mean vector to reorient shapes and conduct a linear comparison (figures 4b and 4f). The second methods translate our function into the frequency domain and compares Fourier modules (figures 4c and

4g). Finally, the third method distinguishes the angles at which ray lengths reach their maximum (figures 4e and 4h).

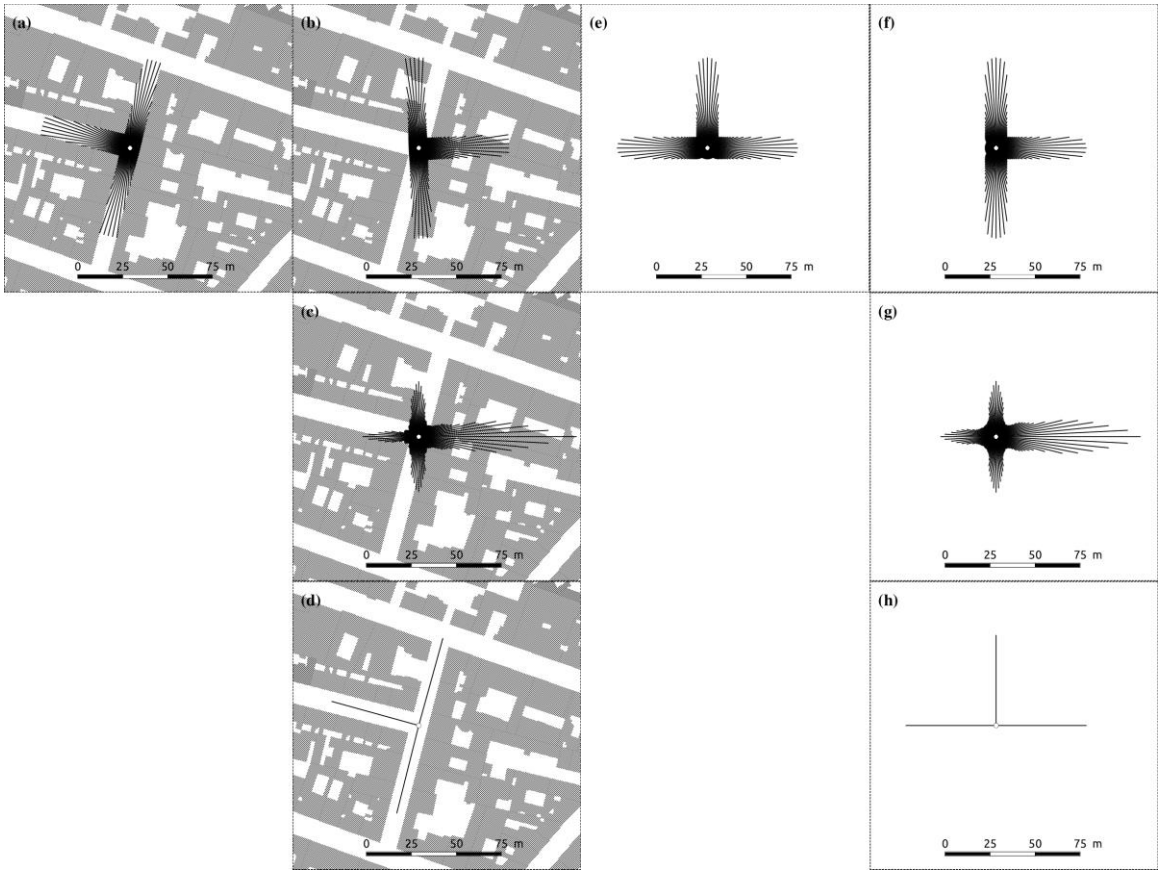

Figure 4: To compare the original signatures of the isovist (a) and the pattern (e), we use three methods: Method 1 - the rectification of the orientation using the mean vector (b and f), Method 2 - the modules of the Fast Fourier Transform (c and g), and Method 3 - the permutation of the mean angular distribution (d and h).

Method 1: Rectification of pattern and isovist orientations using the mean vector

Using the previously established formalism, we may express the mean of all vectors linking the generation point to each contour as:

$$\frac{1}{n}\sum_{k=1}^{n} r_k e^{i\theta_k} = \bar{r}e^{i\bar{\theta}}$$

The form's general orientation given by the mean vector allows us to "rectify" the viewshed (figure 4b). To do so, we position each ray length (i.e. rotation from the East-mean alignment) and subtract the azimuth of the mean vector's using the following formula:

$$\left\{r_k e^{i(\theta_k - \bar{\theta})}\right\}_{k\in\{1,\dots,n\}}$$

If the form is perfectly symmetrical (as for the patterns #20, 43, 45, 63, and 80), the corresponding mean vector is null. We then decide not to apply the rectifying process.

The objective of this rotation is to rectify the studied form by aligning it full-East on the "azimuth of origin" for a direct linear comparison of the visual and geo-spatial patterns.

Method 2: Comparison of the frequency functions using the Discrete Fourier Transform

Method2, using the Fourier Transform traditionally used for time-dependent signals, incorporates a periodic complex-valued function composed of regular angular intervals and their decomposition into a set of sinusoidal functions.

Because the function of radial distances is discrete (due to the implemented underlying ray-casting), we have applied the Python Numpy Fast Fourier Transform (FFT). FTT properties include completeness (it is an invertible and linear transform), periodicity, and shift capability. All three of these properties are essential to describe nearly equivalent shapes, if identically oriented before or after rotation.

To bypass the effects of a form's orientation, we exclude information relative to the angular distribution of the rays by omitting phase, and only consider the distribution of ray lengths given by the FFT modules (figure 4c).

Method 3: Comparison of mean angular distances between peaks

The objective of the third method is to produce a sequence of angular distances between the *extrema* of the form, which are determined by a threshold.

Method 3 first evaluates the mean azimuth of the adjacent ray set qualified as *extremum*. In a second phase, the angular distance between two adjacent azimuths of the mean *extrema* are calculated, starting east and in a counter-clockwise order. In figure 4d, the application of Method3 gives the sequence [91.4°, 178.4°, 90.3°], as the Northern branch is recognized first, followed by the Western and Southern branches. The pertinence of the results, based on threshold value, is therefore dependent on the aforementioned ray length and the threshold ratio.

Measures of similarity and pattern pairing

After deriving the quantitative information from the set of real-world and auto-generated patterns, we assess the level of similarity between the two sets. The pairing consists in identifying the reference form whose distance is smallest from the real-world form (figure 5b). After testing multiple distance methods (Manhattan, Chebyshev, DTW, Canberra), we opted for the L2 Euclidian distance which yielded best results for all three methods.

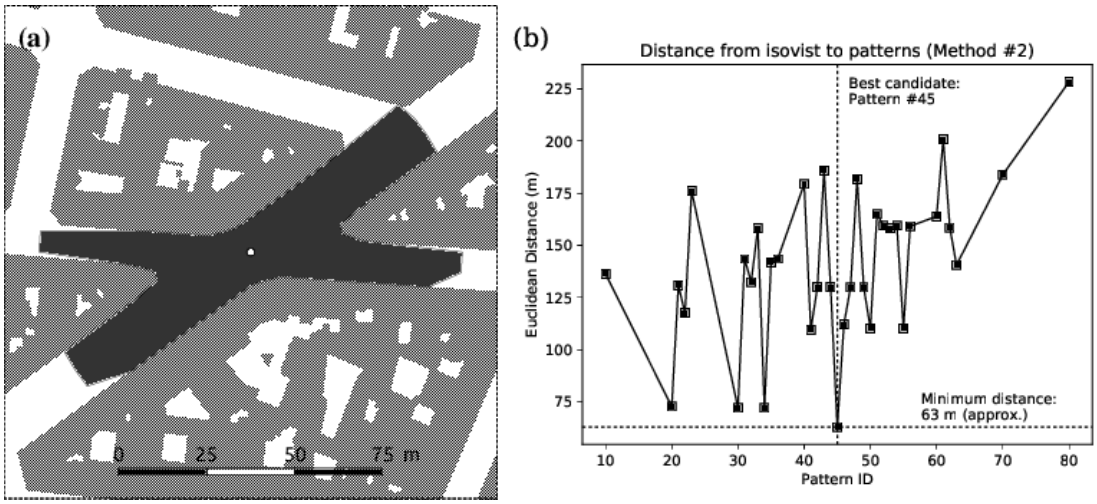

Figure 5: The distance from the actual shape (a) to each of the 35 patterns is evaluated. The pattern selected is the one that minimizes these distances (b).

This pairing necessarily relies on the technique used in the previous step. It is therefore possible to assess the certainty of a result relative to other results found by the same procedure, but there is, as of yet, no suitable solution to compare the certainty of each method in cases of conflicting matches.

Results: Comparison of Use Cases

Three use cases (figure 6) with contrasting morphologies were analyzed. The first one is an area of about 4.6 km² located in Borough Park, Brooklyn, New York. The second use case is a 2 km² wide area located in Le Havre, France, and includes the rebuilt City Center as well as the North East Danton borough. At last, Paris 9th borough, France, is an area of about 2.2 km².

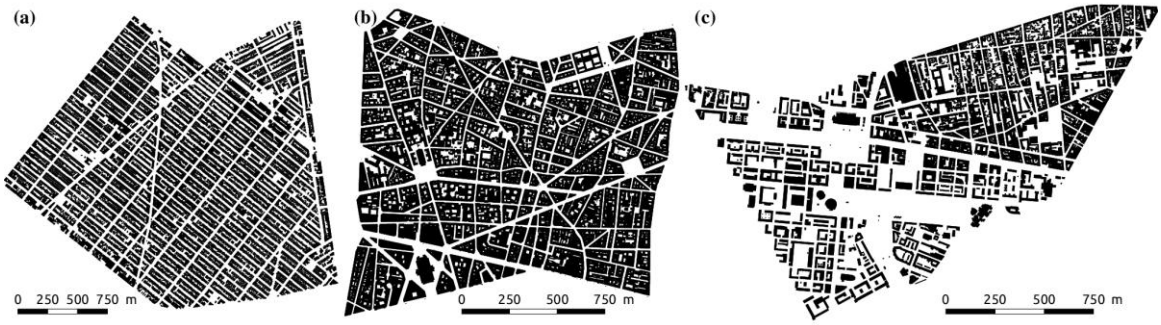

Figure 6: a) Map of Borough Park (New York), b) Map of Paris 9th Borough, c) Map of Le Havre (France).

To assess the reliability of the different methods, each node of each real urban graph was preliminarily manually assessed. This manual classification is called “ground truth”.

The morphology of the streetscape influences the difficulty in assigning an objectively “best pattern”, for several reasons. Firstly, considering different distances from the center point may yield different results. To remedy this ambiguity, we have built a short range ground truth and a long range ground truth assessment representing the possible intersection pattern at different distances. Furthermore, the angularity of certain real intersections may be ambiguously similar to more than one pattern, so much so that differing pattern assignments may be considered equally correct. Finally, the width of

certain streets or plaza openings are also a cause for ambiguous manual assessment, as explained further on in this paper.

As we may notice (see table 1), the first use case (New York borough) is relatively unambiguous, composed mainly of right-angled four-way intersections. Three diagonal roads disturb the orthogonal grid, forming unconventional intersections and plazas. As such, short range and long range assessments are undifferentiated (i.e. we consider that ray length has no influence on expected results).

In contrast, the manual assessment of the second use case (Paris's 9th borough) was much more challenging. Ambiguous intersections were found to be much more prevalent due to the complex morphology. We therefore manually assessed each node considering the immediate (short range) and slightly more distant (long range) streetscape and assigned two possible correct results in 64 out of 335 cases at a short range scale, and 74 out of 335 at a long range scale.

Finally, the Le Havre borough, from which the Lecesne intersection originates, may be considered as an "in-between", as the Southwestern section is composed of an orthogonal grid, and the Northeastern is much more complex. We will notice though, that the orthogonal portions of the streetscape present very large open spaces. As such, the delimitation between "street" and "built environment" is much more ambiguous than the first two use cases. This caused us to consider nearly 37.4% of the intersections as ambiguous at a short range scale and 30.6% at a long range scale.

Table 1: Ratio of ambiguous intersections at both short range and long range scales.

	Number of intersections	Short range scale	Long range scale
New York borough	297		2.7%
Paris's 9th borough	335	19.1%	22.1%
Le Havre borough	444	37.4%	30.7%

Comparing Use Case Results

The three use cases reveal contrasting results for each automatic assessment method. We may first notice that the less complex the urban fabric is, the better the detection rates are (figure 7): 78% success rate for New York (Method 2), 59% for Le Havre (Method 2), and 53% for Paris (Methods 2/3). Furthermore, success rates by ray length (figure 8a) suggest that New York did indeed not need two different scales of evaluation: maximum success rates remain stable for all methods regardless of the distance between center point and viewshed limit. In contrast, when considering the short range interpretations of the other two use cases, success rates for short range interpretations tend to drop and long range success rates tend to rise after a certain ray length.

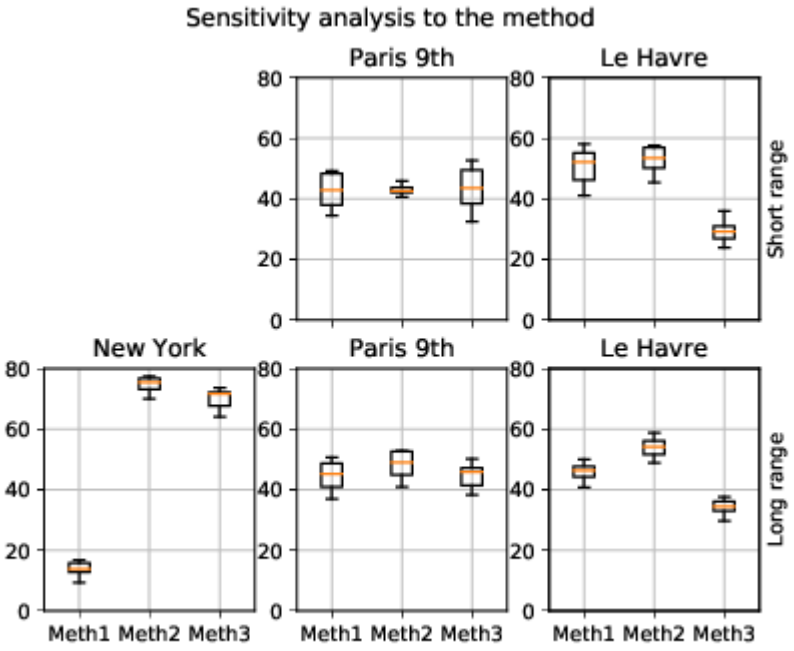

Figure 7: Box plots regarding the pattern matching assessment on the three studied districts.

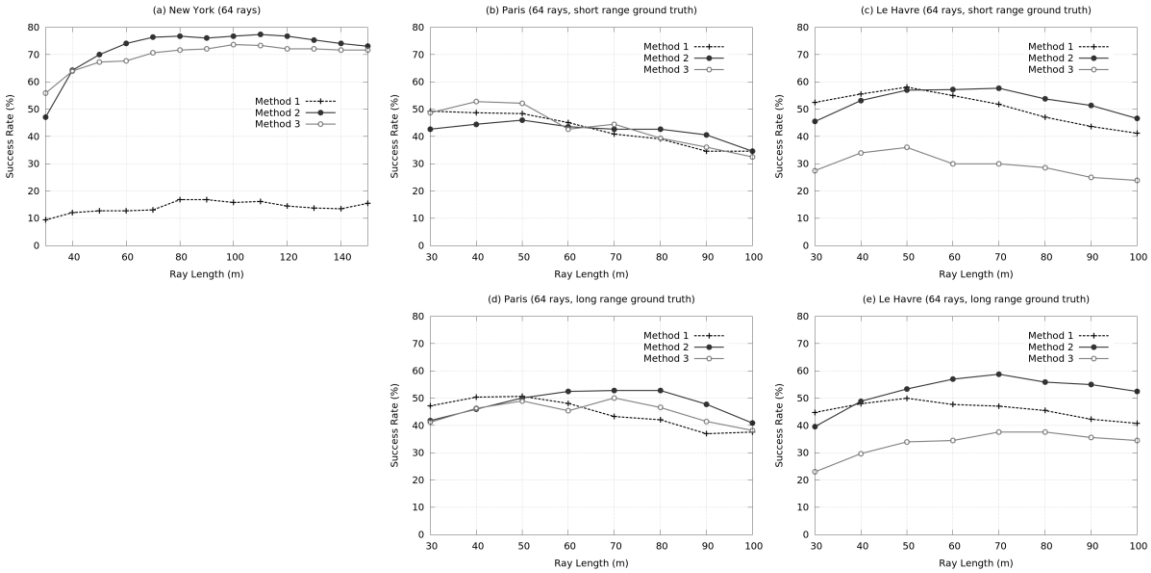

Figure 8: Results of the pattern matching assessment on Borough Park (a), Paris 9th Borough (b and d), and Le Havre (France, c and e).

We may notice though, that Le Havre's long range success rates stagnate whilst Paris's long range success rates present a dip at longer ray lengths. This means that some of Paris's intersections change pattern more than twice when increasing ray length, whilst two scales of interpretation are sufficient for Le Havre. As an example, the junction node #193 in Paris is similar to pattern #30 when the radius length is 30m, to pattern #45 when the radius length is 50m and to pattern #50 when the radius length is 100m (figure 9a). In addition, the threshold at which long range interpretations become more pertinent than short range interpretations is smaller for Paris than for Le Havre.

Furthermore these complex urban fabrics include many curved streets, dead ends, or kiosks which limit isovists' lines of sight. All these obstacles justify the evolution of the success rate curbs at the long range scale. Thus the peak of the long range interpretations ratio at 70-80m (decreasing or increasing the length leads to a deterioration in performance) in Paris 9th borough is clearly due to the fact that the corresponding intersections are tightly clustered and their interpretations vary greatly with ray length. Interpretations are modified when another intersection enters the line of

sight, or when longer ray lengths prematurely end, such as in close-knit, three-way intersections or convoluted spaces such as winding roads.

We can also notice that the ground truth is even questionable. Thus, in New York and for the used dataset, node #87 (figure 9b) has been empirically assimilated to pattern #45 (X-junction). By means of Method 2, we detected it as pattern #43 (right angle crossroads). This "wrong" detection is relative insofar as an ambiguity remains related to the chosen angular distance sampling (which cannot be lower than 45°).

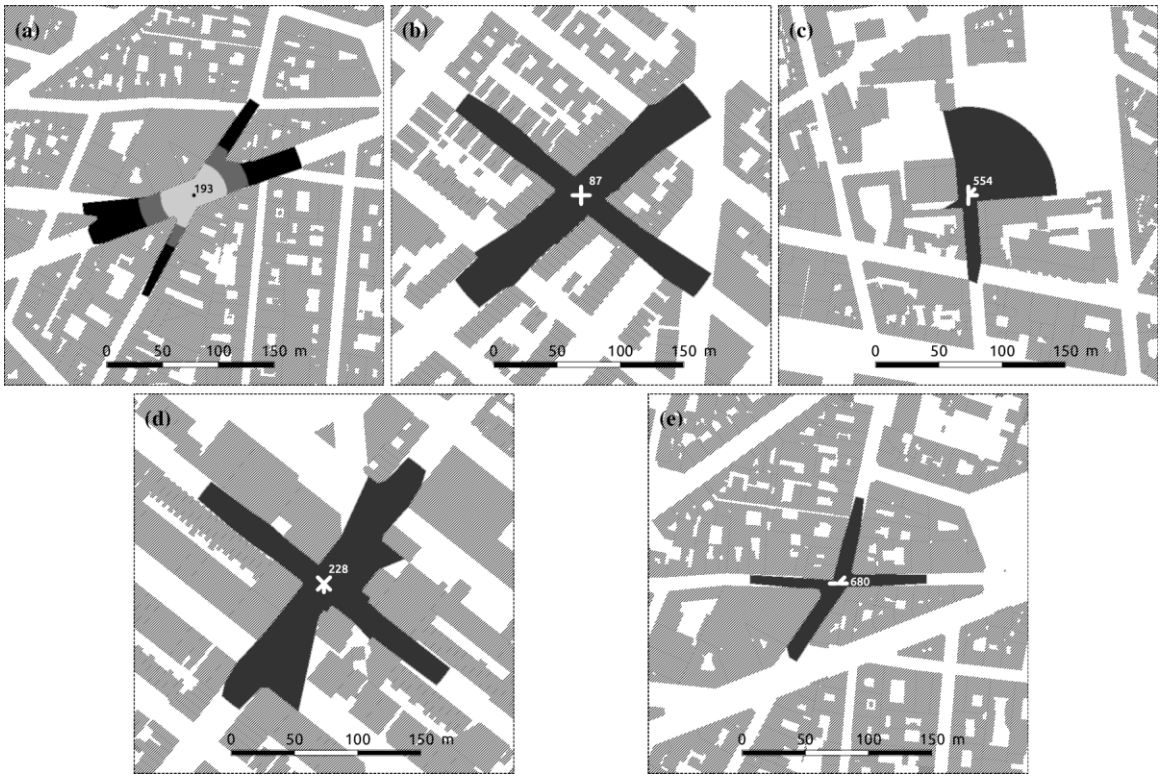

Figure 9: Examples of spatial configurations exhibiting special features.

As an exception to this rule, the Lecesne intersection presented at the beginning of the paper (figure 1) requires a single point with a viewshed of 55 meters for the six branches to be taken into account. A smaller viewshed requires at least two intersection (i.e. generation) points to cover the entire area.

Comparing Method Results

We may first notice that Method 1 yields unsatisfactory results for nearly all terrains, and more especially on the urban fabric composed mainly of right-angled four-way intersections (New York), regardless of ray length. This may be explained by the radial symmetry of many intersections, leading to a null mean vector and therefore the absence of proper rotation, strongly limiting the use of this method. Nonetheless, Method 1 yields satisfactory results on nodes that are not symmetrical.

Method 2 yields the more stable and convincing results on all three terrains. It is able to differentiate streets from large open spaces (plazas), but is sensitive to point position and building geometry such as uneven street widths or curbed streets. Method 3 is quite effective on the very regular urban fabric (New York) and the complex urban morphology (Paris), but does not differentiate between streets and plazas, giving a single mean direction for the opening of the plaza rather than recognizing that the plaza offers multiple directional choices, as Method 2 do. For example, in the case presented in figure 9c, Method 2 will return “Pattern 47” whereas Method 3 will return “Pattern 22”. This explains the rather feeble success rates for Method 3 in Le Havre on a short range scale, which presents a nearly “Corbusean” morphology, with large open spaces separating individual buildings rather that a clear distinction between street and building blocks.

In an effort to reduce calculation times, different numbers of rays were tested. It was found that for all three terrains, at least 64 rays were necessary for the correct approximation of the form, this number growing with ray length so as to keep an acceptable distance between each ray extremity. Otherwise, small branches or buildings may go unnoticed. Inversely, a very high ray count creates noisy signatures, which interferes with all three methods.

Discussion: Unconventional or Ambiguous Intersections

As shown in figure 9d, the detection of junction whose shape is rather evasive nevertheless misleads Method 2. Such junctions, full of ambiguities, probably require an appropriate post processing. In addition, we have already mentioned that using official road dataset may present several disadvantages. Point placement is sometimes inconsistent, there is often a surplus of points for a single intersection area, and points may not be ideally placed (which leads to errors in the interpretation of the junction as

exhibited in figure 9e). The use of a skeleton would reduce the necessary datasets to the single buildings layer. By building the road graph according to the built environment, we hope it will make for fewer, better and more consistently placed points considering the overall visibility of each street from the intersection.

For a further analysis of point location on expected results, we have pinpointed five intersections in the Parisian borough and compared the results of the graphs from the Real Urban Graph (RUG, figure 10a) with OpenStreetMap (OSM, figure 10b) road data and a network created by skeletonization (SKEL, figure 10c).These five intersections are here described by their position: three Northern intersections, including the Center and East intersections which are small and relatively unambiguous, and two southern intersections (east and west) which, like the Northwestern intersection, cover a much larger area and carry a varying number of points in all three networks.

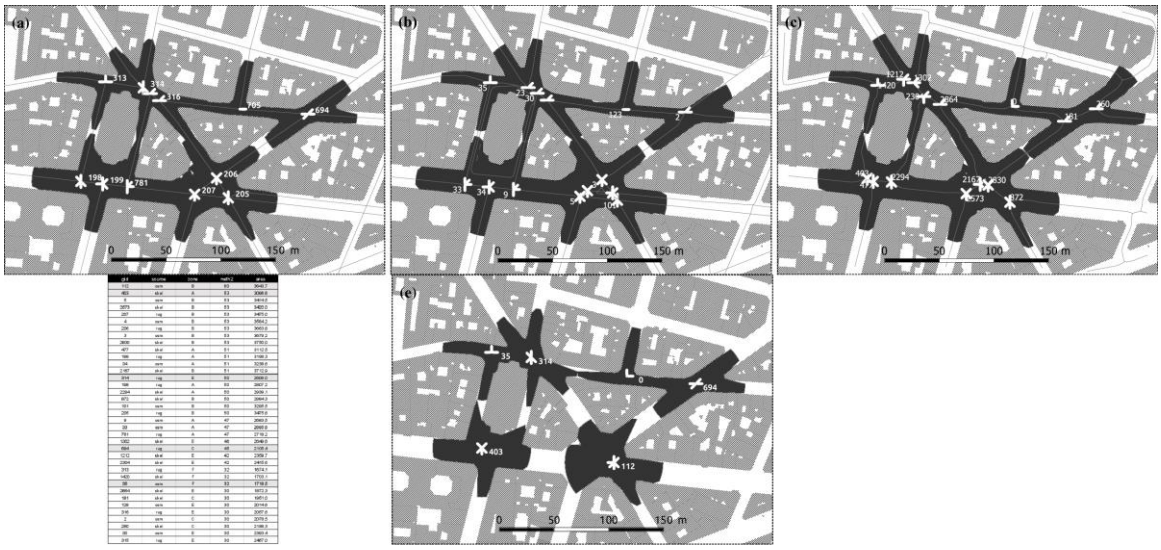

Figure 10: Real Urban Graph (a), OpenStreetMap (b), and Skeleton (c) intersection points as characterized by Method 2 at a line of sight of 45m and with 64 rays. The result of selecting the point at each intersection with the greatest isovist area (e).

The most Northwestern, Southwestern, Southeastern junctions (but also to a lesser extent the Northeastern one) are obviously ambiguous and therefore hard to interpret. Due to misplacement and proliferation, viewpoints have incomplete views of the entire

intersection; their interpretation is therefore incomplete yet coherent considering their local visibility. Identifying unique pattern that correctly agglomerates the information for the entire zone would be a more satisfactory result.

A closer look at the maps, let us think that the viewpoint offering the most complete and appropriate information appears to be the most centered one, such a vantage location would logically offer a simultaneous perspective on multiple branches.

The table presented in figure 10d lists, for each data layer, for each intersection and for each node, the corresponding isovist area. This listing is sorted by decreasing area value. In an effort to join the results of all three graphs, we noticed that the isovists with the largest areas at each intersection were those that gave the most pertinent results (figure 10e). This presumption that intrinsic isovist characteristics may indicate correct point placement needs to be further tested. If this hypothesis were confirmed, we could imagine an empirical research method from the optimal point of view (covering the most of the intersection studied). This heuristic would exploit some simple shape indicators such as area, perimeter or number of concavities.

Conclusion

We have presented three methods to consistently symbolize the open streetscape at urban intersections, based on the comparison of auto-generated patterns and isovist signatures. We have further provided guidelines for the most informative symbolization of the intersection of streets and plazas. We have defined a complex intersection as a concave space where all inlets are not visible at once, and provided orientations towards a way of partitioning such a space. Our case studies have uncovered a correlation between the area's urban morphology and the optimal isovist parameters needed to recognize the correct pattern.

An isovist creates a distinct separable entity to which we may give an identity, including the visual pattern associated with the rest of the atomized plenum. We have found multiple criteria for optimal isovist generation and pattern recognition. Most importantly, ray length and point placement are the two most determining factors in the quality of the results, along with angular distance sampling and the size of the pre-constructed patterns. The values of these four parameters are entirely dependent on the area's urban morphology. We may strongly presume that similar terrains will require similar parametrization.

In the future, legitimate distance measures for direct comparison of the three methods should be determined, to better identify which of the three methods consistently offers more suitable patterns. The method-based differences between matched patterns, as illustrated with differences at corner inlets of plazas, may be resolved by the addition of a new set of geo-spatial patterns taking into account the representation of large openings.

Finally, the question of point placement for the optimal visibility of the most outlets is still open. Several possibilities come to mind, but our research indicates that the centroid of the intersection's kernel, which would lead to the isovist with the largest area, may be an interesting path to pursue. The amount of convex areas within an intersection would then indicate the minimum number of points needed to fully describe the surrounding intersections.

Acknowledgements

The authors would like to thank Michel Leduc, Honorary Professor at the University of Le Havre, France, for his helpful comments and suggestions.

Declaration of conflicting interests

The author(s) declared no potential conflicts of interest with respect to the research, authorship, and/or publication of this article.

Bibliography

Ai T, Cheng X, Liu P, Yang M, 2013, "A shape analysis and template matching of building features by the Fourier transform method" *Computers, Environment and Urban Systems* **41** 219–233, http://linkinghub.elsevier.com/retrieve/pii/S019897151300063X

Benedikt M L, 1979, "To take hold of space: isovists and isovist fields" *Environment and Planning B: Planning and Design* **6**(1) 47–65

Cao, C. and Sun, Y. (2014) 'Automatic Road Centerline Extraction from Imagery Using Road GPS Data', *Remote Sensing*, 6(9), pp. 9014–9033. doi: 10.3390/rs6099014.

Couclelis H, 1992, “People Manipulate Objects (but Cultivate Fields): Beyond the Raster-Vector Debate in GIS”, in *Theories and Methods of Spatio-Temporal Reasoning in Geographic Space, International Conference GIS - From Space to Territory: Theories and Methods of Spatio-Temporal Reasoning* Eds A U Frank, I Campari, and U Formentini Lecture Notes in Computer Science (Springer, Pisa, Italy), pp 65–77

Fisher-Gewirtzman, D. (2018) ‘Integrating “weighted views” to quantitative 3D visibility analysis as a predictive tool for perception of space’, *Environment and Planning B: Urban Analytics and City Science*, 45(2), pp. 345–366. doi: 10.1177/0265813516676486.

Mackaness, W. A. and Mackechnie, G. A. (1999) ‘Automating the Detection and Simplification of Junctions in Road Networks’, *GeoInformatica*, 200, pp. 185–200.

Marshall S, 2005 *Streets & Patterns* (Spon Press, Oxon (UK))

Sarradin F, Siret D, Couprie M, Teller J, 2007, “Comparing Sky Shape Skeletons for the Analysis of Visual Dynamics along Routes” *Environment and Planning B: Planning and Design* **34**(5) 840–857, http://journals.sagepub.com/doi/10.1068/b32143

Steiniger S, 2007 *Enabling pattern-aware automated map generalization*, University of Zürich, Faculty of Science, Institute of Geography.

Teller J, 2003, “A Spherical Metric for the Field-Oriented Analysis of Complex Urban Open Spaces” *Environment and Planning B: Planning and Design* **30**(3) 339–356, http://journals.sagepub.com/doi/10.1068/b12930

Turner A, Doxa M, O’Sullivan D, Penn A, 2001, “From isovists to visibility graphs: a methodology for the analysis of architectural space” *Environment and Planning B: Planning and Design* **28**(1) 103–121

Wang, J., Qin, Q., Gao, Z., Zhao, J. and Ye, X. (2016) ‘A New Approach to Urban Road Extraction Using High-Resolution Aerial Image’, *ISPRS International Journal of Geo-Information*, 5(7), p. 114. doi: 10.3390/ijgi5070114.

Zhang X, Ai T, Stoter J, Kraak M-J, Molenaar M, 2011, “Building pattern recognition in topographic data: examples on collinear and curvilinear alignments” *GeoInformatica*

17(1) 1–33

Zhang X, Luo G, He G, Chen L, 2017, "A Multi-Scale Residential Areas Matching Method Using Relevance Vector Machine and Active Learning" *ISPRS International Journal of Geo-Information* **6**(3) 70, http://www.mdpi.com/2220-9964/6/3/70

Zhou Q, Li Z, 2012, "A comparative study of various strategies to concatenate road segments into strokes for map generalization" *International Journal of Geographical Information Science* **26**(4) 691–715